

## Incorporation of Phosphorus Guest Ions in the Calcium Silicate Phases of Portland Cement from $^{31}\text{P}$ MAS NMR Spectroscopy

Søren L. Poulsen, Hans J. Jakobsen, and Jørgen Skibsted\*

*Instrument Centre for Solid-State NMR Spectroscopy and Interdisciplinary Nanoscience Center (iNANO),  
Department of Chemistry, Aarhus University, DK-8000 Aarhus C, Denmark*

Received January 22, 2010

Portland cements may contain small quantities of phosphorus (typically below 0.5 wt %  $\text{P}_2\text{O}_5$ ), originating from either the raw materials or alternative sources of fuel used to heat the cement kilns. This work reports the first  $^{31}\text{P}$  MAS NMR study of anhydrous and hydrated Portland cements that focuses on the phase and site preferences of the  $(\text{PO}_4)^{3-}$  guest ions in the main clinker phases and hydration products. The observed  $^{31}\text{P}$  chemical shifts (10 to  $-2$  ppm), the  $^{31}\text{P}$  chemical shift anisotropy, and the resemblance of the lineshapes in the  $^{31}\text{P}$  and  $^{29}\text{Si}$  MAS NMR spectra strongly suggest that  $(\text{PO}_4)^{3-}$  units are incorporated in the calcium silicate phases, alite ( $\text{Ca}_3\text{SiO}_5$ ) and belite ( $\text{Ca}_2\text{SiO}_4$ ), by substitution for  $(\text{SiO}_4)^{4-}$  tetrahedra. This assignment is further supported by a determination of the spin–lattice relaxation times for  $^{31}\text{P}$  in alite and belite, which exhibit the same ratio as observed for the corresponding  $^{29}\text{Si}$  relaxation times. From simulations of the intensities, observed in inversion–recovery spectra for a white Portland cement, it is deduced that 1.3% and 2.1% of the Si sites in alite and belite, respectively, are replaced by phosphorus. Charge balance may potentially be achieved to some extent by a coupled substitution mechanism where  $\text{Ca}^{2+}$  is replaced by  $\text{Fe}^{3+}$  ions, which may account for the interaction of the  $^{31}\text{P}$  spins with paramagnetic  $\text{Fe}^{3+}$  ions as observed for the ordinary Portland cements. A minor fraction of phosphorus may also be present in the separate phase  $\text{Ca}_3(\text{PO}_4)_2$ , as indicated by the observation of a narrow resonance at  $\delta(^{31}\text{P}) = 3.0$  ppm for two of the studied cements.  $^{31}\text{P}\{^1\text{H}\}$  CP/MAS NMR spectra following the hydration of a white Portland cement show that the resonances from the hydrous phosphate species fall in the same spectral range as observed for  $(\text{PO}_4)^{3-}$  incorporated in alite. This similarity and the absence of a large  $^{31}\text{P}$  chemical shift anisotropy indicate that the hydrous  $(\text{PO}_4)^{3-}$  species are incorporated in the interlayers of the calcium–silicate–hydrate (C–S–H) phase, the principal phase formed upon hydration of alite and belite.

### Introduction

The global consumption of Portland cement has more than doubled during the past two decades, reflecting its vital role in the house-building industry and the improvement of infrastructures, and it is forecasted that today's cement production will at least double again by the year 2050 to more than 6 billion tonnes per year.<sup>1,2</sup> Roughly 800 kg of  $\text{CO}_2$  is emitted for every tonne of Portland cement produced by today's technologies, amounting to more than 2 billion tonnes per year and resulting in cement production being responsible for about 5% of the global anthropogenic  $\text{CO}_2$  emission. Thus, the cement industry faces an urgent and serious challenge in increasing its production capacity and at the same time

reducing the total  $\text{CO}_2$  emission to meet the world community's regulations.

Roughly 40% of the  $\text{CO}_2$  emitted by cement production results from the fuel used to heat the cement kilns and drive the mills, while 60% originates from the decarbonation of limestone, required to form the main cement clinker phases, i.e., impure forms of alite ( $\text{Ca}_3\text{SiO}_5$ ), belite ( $\text{Ca}_2\text{SiO}_4$ ), tricalcium aluminate ( $\text{Ca}_3\text{Al}_2\text{O}_6$ ), and calcium aluminoferrite ( $\text{Ca}_2\text{Al}_x\text{Fe}_{2-x}\text{O}_5$ ). A direct approach to reduce the  $\text{CO}_2$  emission is the partial replacement of Portland cement by supplementary cementitious materials, for example fly ashes from coal burning, slags from pig iron production, silica fume from the production of ferrosilicon, or natural pozzolans such as volcanic rocks and heat-treated clay minerals. Another approach utilizes biofuels to heat the cement kilns, thereby partly replacing the traditional kiln fuels of gas, oil, and coal. Alternative fuels also include meat and bone meal, sewage sludge, used oils, waste tires, solvents, and a range of other industrial byproducts.<sup>3,4</sup> However, such waste materials may introduce trace elements in the cement that can affect the

\*To whom correspondence should be addressed. Phone: (+45) 89423900. Fax: (+45) 86196199. E-mail: jskib@chem.au.dk.

(1) U.S. Department of the Interior, U.S. Geological Survey. *Mineral Commodity Summaries 2009*; United States Government Printing Office: Washington DC, 2009.

(2) Damtoft, J. S.; Lukasik, J.; Herfort, D.; Sorrentino, D.; Gartner, E. M. *Cem. Concr. Res.* **2008**, *38*, 115–127.

**Table 1.** Bulk Oxide Composition (wt %) for the Studied Portland Cements from XRF Analysis and Quantities (wt %) of Alite and Belite Determined from  $^{29}\text{Si}$  MAS NMR Spectroscopy<sup>a</sup>

cement	CaO	SiO <sub>2</sub>	Al <sub>2</sub> O <sub>3</sub>	Fe <sub>2</sub> O <sub>3</sub>	MgO	SO <sub>3</sub>	K <sub>2</sub> O	Na <sub>2</sub> O	P <sub>2</sub> O <sub>5</sub>	alite <sup>b</sup>	belite <sup>b</sup>
A	68.67	24.68	2.11	0.43	0.58	1.82	0.06	0.17	0.45	72.4	20.0
B	61.29	20.51	5.10	3.33	2.82	2.78	1.40	0.24	0.37	59.1	17.4
C	64.18	21.01	4.63	2.60	1.82	2.78	0.94	0.20	0.40	62.4	16.4
D	63.45	21.03	5.01	2.54	2.05	3.01	1.02	0.26	0.08	70.3	10.2

<sup>a</sup> The cements A–D are identical to cements A–D in a recent  $^{29}\text{Si}$  MAS NMR and powder X-ray diffraction investigation focusing on the quantification of alite and belite by different approaches.<sup>23</sup> Cement A is a white Portland cement, and cements B–D are ordinary Portland cements. <sup>b</sup> It is assumed that alite and belite have the average compositions proposed by Taylor.<sup>24</sup>

grindability of the clinkers, the reactivity (hydration reactions), and the durability of the resulting cement.<sup>5,6</sup> Thus, it is important to study the chemical impact of these guest ions on the main Portland clinker phases in relation to applications of alternative fuels. For example, the use of meat and bone meal or sewage sludge as alternative fuels may result in the incorporation of a significant amount of phosphorus in the cement, corresponding to a bulk content roughly in the range 0.1–0.6 wt %  $\text{P}_2\text{O}_5$ .<sup>7</sup>

Earlier studies have shown that phosphorus ( $\text{P}^{5+}$  in  $(\text{PO}_4)^{3-}$  ions) mainly enters the calcium silicate phases with a preferential formation of a phosphatic belite solid solution for phosphorus concentrations above 1 wt %  $\text{P}_2\text{O}_5$ .<sup>8,9</sup> The upper limit for incorporation of phosphate ions in alite has been reported to be 1.1 wt %  $\text{P}_2\text{O}_5$ ,<sup>9</sup> corresponding to a molar P/Si ratio of 0.036. Furthermore, incremental addition of  $\text{P}_2\text{O}_5$  results in a progressive reduction in the alite content, corresponding to 9.9 wt % per added 1 wt % of  $\text{P}_2\text{O}_5$ ,<sup>8</sup> which significantly reduces the mechanical strength of the resulting hydrated Portland cement. Phosphate contents above 1.0 wt %  $\text{P}_2\text{O}_5$  are found only in cements produced from phosphatic limestone deposits in certain parts of the world. Thus, more recent research has focused on effects from small amounts of phosphate on the cement clinking processes and hydraulic reactivities,<sup>7,10–14</sup> which are more realistic conditions for the clinker burning in an industrial kiln where a significant (e.g., 20%) part of the conventional fuel is replaced by meat and bone meal. For a laboratory-made clinker containing 0.6 wt %  $\text{P}_2\text{O}_5$ , X-ray microanalysis indicated that a maximum of 2.3% and 3.3% of the silicon sites can be replaced by phosphorus in alite and belite, respectively.<sup>7</sup> Other studies have investigated the coupled incorporation of  $(\text{PO}_4)^{3-}$  and a trivalent metal ion ( $\text{Al}^{3+}$ ,  $\text{Mn}^{3+}$ ,  $\text{Fe}^{3+}$ ,  $\text{Cr}^{3+}$ ) for synthetic phases of alite<sup>10,14</sup> and belite<sup>11–13</sup> with the principal aim of

identifying polymorphic changes and transformations from alite to belite and  $\text{CaO}$  phases.

In this work we report the first application of solid-state  $^{31}\text{P}$  magic-angle spinning (MAS) nuclear magnetic resonance (NMR) spectroscopy in cement chemistry by the detection of phosphorus guest ions in anhydrous and hydrated production Portland cements containing bulk phosphorus contents in the range 0.08–0.45 wt %  $\text{P}_2\text{O}_5$ . Generally, the local environment of  $(\text{PO}_4)^{3-}$  ions in cement minerals is difficult to characterize by conventional analytical techniques, such as powder X-ray diffraction, as a result of the low concentration and presumed random distribution over several lattice sites. The present work utilizes the very favorable NMR properties of the  $^{31}\text{P}$  spin, i.e., nuclear spin  $I = 1/2$ , high Larmor frequency, and 100% natural abundance, as well as results from earlier studies of inorganic phosphates, which have revealed that the phosphate  $^{31}\text{P}$  NMR chemical shifts primarily depend on the local structural environments of the  $\text{PO}_4$  species.<sup>15,16</sup> The observed  $^{31}\text{P}$  chemical shifts, chemical shift anisotropies, and spin–lattice relaxation times, along with  $^{31}\text{P}\{^1\text{H}\}$  cross-polarization (CP) MAS NMR experiments for the hydrated samples, provide structural information about phase and site preferences of the phosphorus guest ions.  $^{31}\text{P}$  MAS NMR has been widely used in inorganic chemistry, including applications that focus on small quantities of phosphate such as phosphorus-modified alumina supports for heterogeneous catalysts<sup>17</sup> and phosphorus incorporated in silicious ZSM-5 zeolites<sup>18,19</sup> and the  $\text{SiO}_2$  polymorph stishovite.<sup>20</sup> In cases where these materials contain significant amounts of phosphorus (> 2 wt %  $\text{P}_2\text{O}_5$ ), heteronuclear correlation NMR experiments such as  $^{31}\text{P}$ – $^{27}\text{Al}$  REDOR/TRAPDOR<sup>21</sup> and  $^{27}\text{Al}$ – $^{31}\text{P}$  CP-HECTOR<sup>22</sup> have been utilized to obtain further information on the local environments of the  $(\text{PO}_4)^{3-}$  ions.

## Experimental Section

**Materials.** Four commercial Portland cements (A–D) obtained from four European cement manufacturers were

- (3) Mokrzycki, E.; Uliasz-Bohenczyk, A. *Appl. Energy* **2003**, *74*, 95–100.
- (4) Kääntee, U.; Zevenhoven, R.; Backman, R.; Hupa, M. *Fuel Process. Technol.* **2004**, *85*, 293–301.
- (5) Trezza, M. A.; Scian, A. N. *Cem. Concr. Res.* **2005**, *35*, 438–444.
- (6) Opoczky, L.; Gavel, V. *Int. J. Miner. Process.* **2004**, *74S*, S129–S136.
- (7) Nastac, D. C.; Kääntee, U.; Liimatainen, J.; Hupa, M.; Muntean, M. *Adv. Cem. Res.* **2007**, *19*, 93–100.
- (8) Nurse, R. W. *J. Appl. Chem.* **1952**, *2*, 708–716.
- (9) Gutt, W. *Proceedings of the 5th International Congress on Cement Chemistry*; Tokyo, Oct. 7–11, 1968, Onogi Shigeharu, Japan, 1968; Vol. I, pp 93–105.
- (10) Diouri, A.; Boukhari, A.; Aride, J.; Puertas, F.; Vazquez, T. *Cem. Concr. Res.* **1997**, *27*, 1203–1212.
- (11) Qotaibi, Z.; Diouri, A.; Boukhari, A.; Aride, J.; Rogez, J.; Castanet, R. *World Cem.* **1999**, *30*, 77–80.
- (12) Fukuda, K.; Taguchi, H. *Cem. Concr. Res.* **1999**, *29*, 503–506.
- (13) Benarchid, M.Y.; Diouri, A.; Boukhari, A.; Aride, J.; Rogez, J.; Castanet, R. *Cem. Concr. Res.* **2004**, *34*, 1873–1879.
- (14) Noirfontaine, M.-N.; Tusseau-Nenez, S.; Signes-Frehel, M.; Gasecki, G.; Girod-Labianca, C. *J. Am. Ceram. Soc.* **2009**, *92*, 2337–2344.

- (15) Turner, G. L.; Smith, K. A.; Kirkpatrick, R. J.; Oldfield, E. J. *Magn. Reson.* **1986**, *70*, 408–415.
- (16) Hartmann, P.; Vogel, J.; Schnabel, B. *J. Magn. Reson. Ser. A* **1994**, *111*, 110–114.
- (17) DeCanio, E. C.; Edwards, J. C.; Scalzo, T. R.; Storm, D. A.; Bruno, J. W. *J. Catal.* **1991**, *132*, 498–511.
- (18) Caro, J.; Bülow, M.; Derewinski, M.; Haber, J.; Hunger, M.; Kärger, J.; Pfeifer, H.; Storek, W.; Zibrowius, B. *J. Catal.* **1990**, *124*, 367–375.
- (19) Seo, G.; Ryoo, R. *J. Catal.* **1990**, *124*, 224–230.
- (20) Stebbins, J. F.; Kim, N.; Brunet, F.; Irifune, T. *Eur. J. Mineral.* **2009**, *21*, 667–671.
- (21) van Eck, E. R. H.; Kentgens, A. P. M.; Kraus, H.; Prins, R. *J. Phys. Chem.* **1995**, *99*, 16080–16086.
- (22) Damodaran, K.; Wiench, J. W.; Cabral de Menezes, S. M.; Lam, Y. L.; Trebosc, J.; Amoureux, J.-P.; Pruski, M. *Microporous Mesoporous Mater.* **2006**, *95*, 296–305.

studied as received. Bulk chemical compositions were obtained by X-ray fluorescence (XRF) analysis and are summarized in Table 1 along with the quantities of alite and belite, determined recently by  $^{29}\text{Si}$  MAS NMR in a study including the same cements.<sup>23</sup> The sample of  $\text{Ca}_3(\text{PO}_4)_2$  was obtained from VWR International (BDH Prolabo, Leuven, Belgium).

A series of hydrated samples were prepared for cement A using a water/cement ratio of 0.4. The cement and water were mixed at 500 rpm for 3 min (motorized stirrer), followed by a rest period of 2 min and then stirring at 2000 rpm for 3 min. The resulting paste was cast in a capped plastic container (50 mL), and after 24 h the paste was demolded and immersed in a closed plastic container (500 mL) filled with tap water. The container was stored in a temperature-controlled room at  $21 \pm 2^\circ\text{C}$ . At appropriate time intervals  $\sim 5$  g of sample was ground to a fine powder and the hydration was stopped by mixing the material with 50 mL of isopropyl alcohol (99%) for 1 h using a magnetic stirrer. Finally, the powder was dried over silica gel in a desiccator for 24 h.

**NMR Measurements.** Solid-state  $^{31}\text{P}$  MAS,  $^{31}\text{P}\{^1\text{H}\}$  CP/MAS, and  $^{29}\text{Si}\{^{31}\text{P}\}$  CP/MAS NMR experiments were performed on a Varian INOVA-400 spectrometer (9.4 T), using a home-built CP/MAS probe for 5 mm o.d. zirconia (PSZ) rotors (110  $\mu\text{L}$  sample volume), or on a Varian Direct Drive VNMR-600 spectrometer (14.1 T), employing a Varian/Chemagnetics triple-resonance T3MAS probe for 4 mm o.d. PSZ rotors (82  $\mu\text{L}$  sample volume). The single-pulse and inversion–recovery  $^{31}\text{P}$  MAS NMR spectra acquired at 9.4 T used an rf field strength of  $\gamma B_1/2\pi = 60$  kHz, the spinning speed  $\nu_R = 12.0$  kHz, a relaxation delay of 60 s, and typically 1000 scans. The  $^{31}\text{P}\{^1\text{H}\}$  CP/MAS experiments (9.4 T) were performed at a moderate spinning speed ( $\nu_R = 5$  kHz), using rf field strengths of  $\gamma B_2/2\pi = 52$  kHz for the initial  $^1\text{H}$  90° pulse and  $^1\text{H}$  decoupling, and  $\gamma B_1/2\pi \approx \gamma B_2/2\pi \approx 45$  kHz for the Hartmann–Hahn match. The  $^{31}\text{P}$  MAS and  $^{29}\text{Si}\{^{31}\text{P}\}$  CP/MAS NMR experiments acquired at 14.1 T in  $^{29}\text{Si}$ – $^{31}\text{P}$  double-tune mode employed a  $^{31}\text{P}$  rf field strength of  $\gamma B_1/2\pi = 60$  kHz and matched  $^{29}\text{Si}$ ,  $^{31}\text{P}$  rf field strengths of  $\gamma B_1/2\pi \approx \gamma B_2/2\pi \approx 40$  kHz, respectively.

$^{31}\text{P}$  chemical shifts are referenced to 85%  $\text{H}_3\text{PO}_4$  using a solid sample of  $(\text{NH}_4)_2\text{HPO}_4$  as a secondary reference ( $\delta_{\text{iso}} = 1.37$  ppm). The chemical shift anisotropy (CSA) parameters ( $\delta_\sigma$  and  $\eta_\sigma$ ) are defined from the principal elements ( $\delta_{ii}$ ) of the CSA tensor as  $\delta_\sigma = \delta_{\text{iso}} - \delta_{33}$  and  $\eta_\sigma = (\delta_{11} - \delta_{22})/\delta_\sigma$ , where  $\delta_{\text{iso}} = 1/3(\delta_{11} + \delta_{22} + \delta_{33})$  following the convention  $|\delta_{33} - \delta_{\text{iso}}| \geq |\delta_{11} - \delta_{\text{iso}}| \geq |\delta_{22} - \delta_{\text{iso}}|$ .

## Results and Discussion

**$^{31}\text{P}$  MAS NMR of Anhydrous Cements.** Four different Portland cements, including a white Portland cement with a low iron content (cement A) and three ordinary Portland cements (cement B–D, cf., Table 1), are studied in the present work. The  $^{31}\text{P}$  MAS NMR spectra of these cements (Figure 1) all exhibit isotropic resonances in the range 10 to  $-2$  ppm with only low-intensity spinning sidebands (not shown) at the present spinning speed ( $\nu_R = 12.0$  kHz) and magnetic field strength (9.4 T). The isotropic  $^{31}\text{P}$  chemical shifts suggest that phosphorus in the anhydrous cements is present as orthophosphate units, following the exploratory  $^{31}\text{P}$  NMR study of orthophosphates by Turner et al.,<sup>15</sup> who found that the isotropic chemical shifts for these  $\text{PO}_4$  units primarily depend on next-nearest neighbor interactions and reported linear correlations between  $\delta_{\text{iso}}(^{31}\text{P})$  and the electronegativity

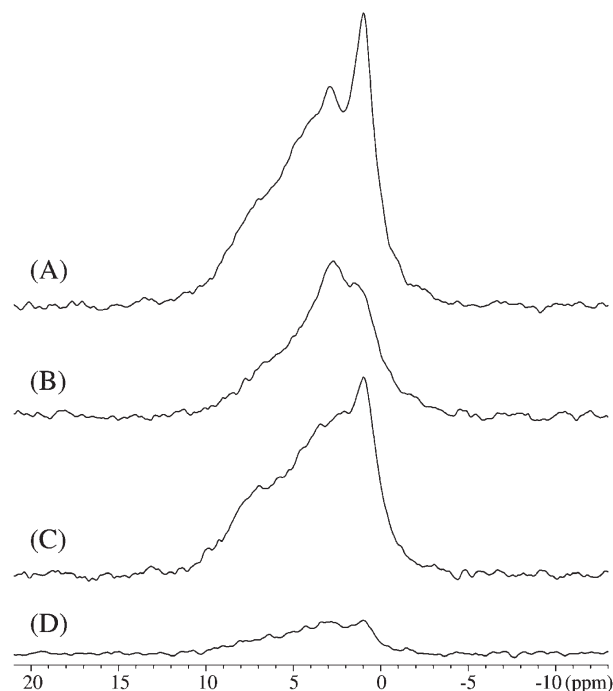


**Figure 1.**  $^{31}\text{P}$  MAS NMR spectra (9.4 T) of the anhydrous Portland cements (A, B, C, and D), obtained with a spinning speed of  $\nu_R = 12.0$  kHz, a 60 s relaxation delay, and 1000–4300 scans. The spectra are shown with the same vertical expansion, and thereby the intensities reflect the bulk content of phosphorus in the cements.

as well as the cation potential ( $Z/r$  where  $Z$  is the cation charge and  $r$  its ionic radius). In agreement with these correlations,  $\delta_{\text{iso}} = 3.0$  ppm was reported for  $\text{Ca}_3(\text{PO}_4)_2$ ,<sup>15</sup> which falls in the same spectral range as the chemical shifts observed for the anhydrous Portland cements. The chemical shift is supported by a  $^{31}\text{P}$  MAS NMR spectrum of  $\text{Ca}_3(\text{PO}_4)_2$ , recorded in this work at 14.1 T (not shown), which reveals a single resonance at  $\delta_{\text{iso}} = 2.8 \pm 0.1$  ppm with a line width of  $\text{fwhm} = 1.1$  ppm. In contrast, condensed aluminum orthophosphate ( $\text{AlPO}_4$ ) resonates at lower frequency ( $\delta_{\text{iso}} = -24.5$  ppm)<sup>15</sup> and in the chemical shift range observed for  $\text{PO}_4$  tetrahedra in framework aluminophosphates (roughly  $-5$  to  $-35$  ppm).<sup>25–27</sup> These variations in  $^{31}\text{P}$  chemical shifts suggest that the phosphorus guest ions are incorporated in the calcium silicate phases alite and belite, which both include orthosilicate  $\text{SiO}_4$  units only,<sup>28,29</sup> rather than in tricalcium aluminate, containing 6-rings of  $\text{AlO}_4$  tetrahedra,<sup>30</sup> or in the calcium aluminoferrite phase with a structure of alternating Fe-rich octahedral and Al-rich tetrahedral layers.<sup>31</sup> Obviously, this assignment assumes that the  $(\text{PO}_4)^{3-}$  ions replace the high-valent  $(\text{SiO}_4)^{4-}$  ions in alite and belite or  $(\text{AlO}_4)^{5-}$  and  $(\text{AlO}_4)^{5-}/(\text{FeO}_6)^{9-}$  in tricalcium aluminate and ferrite, respectively.

(25) Blackwell, C. S.; Patton, R. L. *J. Phys. Chem.* **1984**, *88*, 6135–6139.

(26) Martens, J. A.; Feijen, E.; Lievens, J. L.; Grobet, P. J.; Jacobs, P. A. *J. Phys. Chem.* **1991**, *95*, 10025–10031.

(27) Fyfe, C. A.; Meyer zu Altenschildesche, H.; Wong-Moon, K. C.; Grondy, H.; Chezeau, J. M. *Solid State Nucl. Magn. Reson.* **1997**, *9*, 97–106.

(28) Nishi, F.; Takeuchi, Y.; Maki, I. *Zeit. Kristallogr.* **1985**, *172*, 297–314.

(29) Jost, K. H.; Zeimer, B.; Seydel, R. *Acta Crystallogr.* **1977**, *B33*, 1696–1700.

(30) Mondal, P.; Jeffery, J. W. *Acta Crystallogr.* **1975**, *B31*, 689–697.

(31) Colville, A. A.; Geller, S. *Acta Crystallogr.* **1972**, *B28*, 3196–3200.

(23) Poulsen, S. L.; Kocaba, V.; Le Saoût, G.; Jakobsen, H. J.; Scrivener, K. L.; Skibsted, J. *Solid State Nucl. Magn. Reson.* **2009**, *36*, 32–44.

(24) Taylor, H. F. W. *Adv. Cem. Res.* **1989**, *2*, 73–77.



The incorporation of  $(\text{PO}_4)^{3-}$  ions in the ferrite phase would imply a loss in  $^{31}\text{P}$  NMR signal intensity from these sites as a result of the strong dipolar interaction between the unpaired electrons of the  $\text{Fe}^{3+}$  ions and the  $^{31}\text{P}$  nuclear spins. However, the fact that the quantity of the ferrite phase in cement A is very low (below 0.5 wt % according to powder X-ray diffraction combined with Rietveld refinement) and that the relative intensities of the  $^{31}\text{P}$  MAS NMR spectra in Figure 1 agree well with the bulk contents of  $\text{P}_2\text{O}_5$  in the cements (Table 1) strongly suggests that an appreciable amount of  $(\text{PO}_4)^{3-}$  ions are not incorporated in the ferrite phase.

The crystal structure for belite ( $\beta\text{-Ca}_2\text{SiO}_4$ )<sup>27</sup> includes a unique Si site, whereas 18 distinct Si atoms are reported for the monoclinic  $M_{\text{III}}$  form of alite.<sup>28</sup> Thus, the replacement of  $(\text{SiO}_4)^{4-}$  by  $(\text{PO}_4)^{3-}$  in belite should result in a single  $^{31}\text{P}$  resonance, whereas a number of overlapping peaks are expected for  $(\text{PO}_4)^{3-}$  ions incorporated in alite. The spectral effects from these substitutions are similar to those observed in an earlier study on the incorporation of  $\text{Al}^{3+}$  guest ions in the two calcium silicate phases by  $^{27}\text{Al}$  MAS NMR,<sup>32</sup> where a single second-order quadrupolar line shape was observed for tetrahedrally coordinated aluminum in belite, while the spectrum of a synthetic  $\text{Ca}_3\text{SiO}_5$  sample doped with  $\text{Al}^{3+}$  revealed a number of overlapping resonances originating from different  $\text{AlO}_4$  sites.

The  $^{31}\text{P}$  MAS NMR spectra of the cements in Figure 1 exhibit the same overall spectral features in the range 10 to  $-2$  ppm, as even observed for the cement with the lowest quantity of phosphorus (cement D, 0.08 wt %  $\text{P}_2\text{O}_5$ ). A narrow resonance at  $\delta(^{31}\text{P}) = 1.0$  ppm is clearly observed for cements A and C, which can also be identified in the spectra of cements B and D. This resonance is tentatively assigned to  $(\text{PO}_4)^{3-}$  ions replacing the unique  $(\text{SiO}_4)^{4-}$  site in belite, while the underlying resonances in the range from 10 to  $-2$  ppm are ascribed to  $(\text{PO}_4)^{3-}$  ions that substitute for the different Si sites in monoclinic  $M_{\text{III}}$  alite. A distinct resonance is also apparent for cements A and B at  $\delta(^{31}\text{P}) = 3.0$  ppm, which is very close to the chemical shift value for  $\text{Ca}_3(\text{PO}_4)_2$  ( $\delta_{\text{iso}} = 2.8$  ppm). Thus, it cannot be excluded that cements A and B include a very small quantity of  $\text{Ca}_3(\text{PO}_4)_2$ ; that is, the intensity of the peak at 3.0 ppm constitutes less than 5% and 10% of the overall  $^{31}\text{P}$  NMR intensity for cements A and B, respectively. Alternatively, differences in the local environments for the individual  $\text{SiO}_4$  tetrahedra may result in a site preference for the  $(\text{SiO}_4)^{4-} \rightarrow (\text{PO}_4)^{3-}$  substitution, which may account for the peak at  $\delta(^{31}\text{P}) = 3.0$  ppm. The overall line shape of the resonances in the range 10 to  $-2$  ppm, beneath the peak from belite at 1.0 ppm, shows some resemblance to the line shape for the overlapping  $^{29}\text{Si}$  resonances in the  $^{29}\text{Si}$  MAS NMR spectra of alite,<sup>23,33</sup> which further support the assignment. The highest intensity for the  $^{31}\text{P}$  resonance from belite is observed for cement A (Figure 1), which also includes the largest belite content of the four studied cements (Table 1). However, the  $^{31}\text{P}$  MAS NMR spectra of cements B and C show a

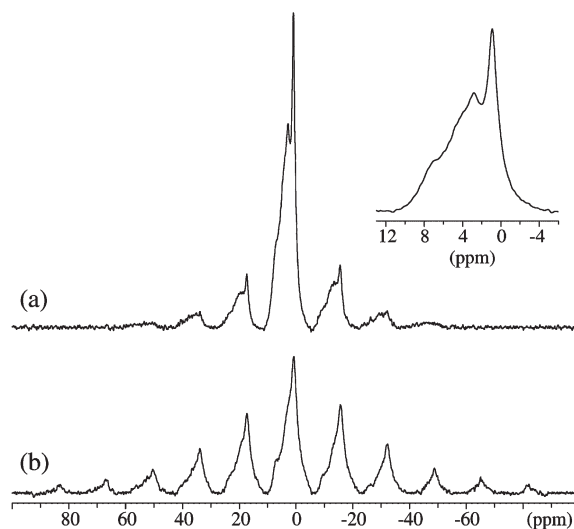


**Figure 2.**  $^{31}\text{P}$  MAS NMR spectra of (a) cement A and (b) cement C recorded at 14.1 T using a spinning speed of  $\nu_R = 4.0$  kHz, a  $90^\circ$  excitation pulse, a 15 s relaxation delay, and (a) 10000 and (b) 5360 scans. The inset illustrates the isotropic peaks for cement A.

significantly larger amount of  $(\text{PO}_4)^{3-}$  guest ions in the belite phase for cement C as compared to cement B, although these cements contain very similar quantities of belite. This indicates that other factors such as the thermal history, the source of phosphorus in the raw materials/fuels, and the content of other minor elements may influence the degree of  $(\text{PO}_4)^{3-}$  ion incorporation in the individual phases of alite and belite.

**$^{31}\text{P}$  Chemical Shift Anisotropy.**  $^{31}\text{P}$  MAS NMR spectra at a higher magnetic field (14.1 T) and lower spinning speed ( $\nu_R = 4.0$  kHz) have also been obtained for the four anhydrous cements (Figure 2). The spectra of cements B–D are rather similar (thus, the spectrum is shown only for cement C) and differ from cement A by a larger number of spinning sidebands (ssbs). The difference in number of ssbs and their intensities for cements A and C reflects the variation in paramagnetic ions (principally  $\text{Fe}^{3+}$ ) and thereby the higher bulk  $\text{Fe}_2\text{O}_3$  contents for cements B–D as compared to cement A (Table 1). Following our recent  $^{29}\text{Si}$  NMR study of paramagnetic ions in the alite and belite phases of anhydrous cements,<sup>23</sup> the larger number and high-intensity ssbs observed for cement C (Figure 2b) are caused by the dipolar interaction between the unpaired electrons of the  $\text{Fe}^{3+}$  ions and the  $^{31}\text{P}$  nuclear spins, which is strongly dependent on the distance between the spins and thereby the concentration of  $\text{Fe}^{3+}$  species in the anhydrous phases. The significantly smaller  $\text{Fe}_2\text{O}_3$  content in cement A implies that the few ssbs observed in the  $^{31}\text{P}$  MAS NMR spectrum (Figure 2a) mainly result from the  $^{31}\text{P}$  chemical shift anisotropy interaction. Employing this assumption and the consideration of only the  $^{31}\text{P}$  CSA interaction in simulations of the centerband and ssb intensities for  $^{31}\text{P}$  in alite and belite, estimated from the spectrum in Figure 2a, the two different types of  $^{31}\text{P}$  environments exhibit shift anisotropies ( $\delta_\sigma$ ) of magnitudes in the ranges  $|\delta_\sigma| = 25\text{--}30$  ppm and  $|\delta_\sigma| = 22\text{--}25$  ppm for  $^{31}\text{P}$  in alite and belite, respectively. Obviously, these values for the anisotropies are upper limits, since  $\text{Fe}^{3+}\text{--}^{31}\text{P}$  electron–nuclear spin dipolar couplings may also contribute slightly to the ssb

(32) Skibsted, J.; Jakobsen, H. J.; Hall, C. J. *Chem. Soc., Faraday Trans.* 1994, 90, 2095–2098.

(33) Skibsted, J.; Jakobsen, H. J.; Hall, C. J. *Chem. Soc., Faraday Trans.* 1995, 91, 4423–4430.

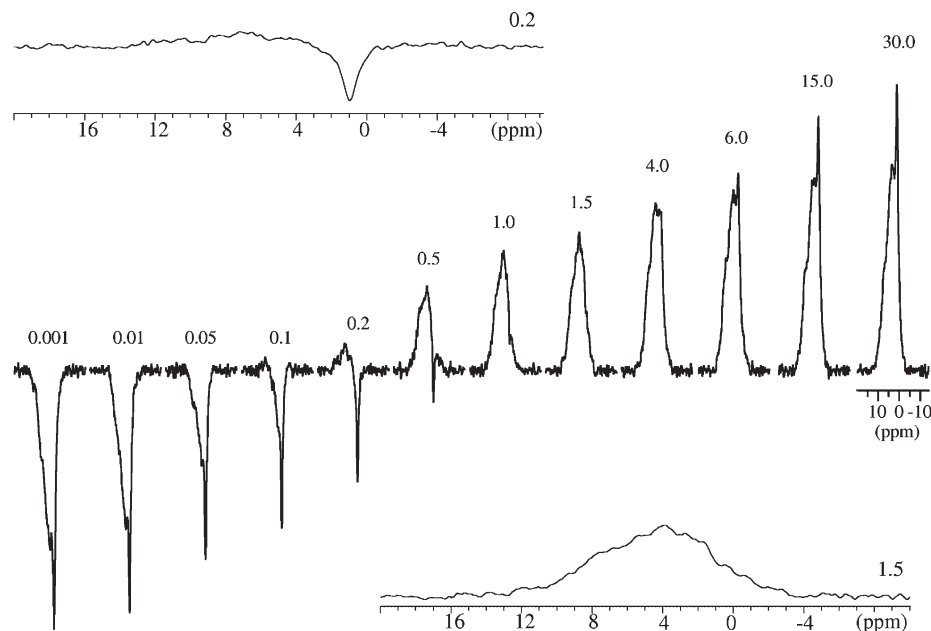


**Figure 3.** Inversion–recovery  $^{31}\text{P}$  MAS NMR spectra (9.4 T,  $\nu_R = 12.0$  kHz) for cement A, illustrating the difference in spin–lattice relaxation for the  $(\text{PO}_4)^{3-}$  guest ions in alite and belite. The expansions above and below the array of spectra correspond to the zero-crossings for  $^{31}\text{P}$  in alite and belite at recovery times of 0.2 and 1.5 s, respectively. The recovery times (in seconds) are indicated for the individual spectra.

intensities. The small values for the shift anisotropies further support the presence of  $^{31}\text{P}$  in isolated  $\text{PO}_4$  tetrahedra since orthophosphate units generally exhibit small shift anisotropies as compared to pyro- and metaphosphates, i.e., magnitudes of  $\delta_\sigma$  below 40 ppm are typical for nonprotonated orthophosphates<sup>16</sup> while  $\delta_\sigma = -110$  to  $-50$  ppm and  $\delta_\sigma = 100$ – $170$  ppm are common for pyro- and metaphosphate  $\text{PO}_4$  units.<sup>16,34</sup>

**Inversion–Recovery  $^{31}\text{P}$  MAS NMR.** A distinction of the  $^{31}\text{P}$  resonances from the  $(\text{PO}_4)^{3-}$  guest ions in alite and belite may be achieved from a difference in spin–lattice relaxation for these species. Thus, the anhydrous cement with the most clear reflection of the resonance from  $^{31}\text{P}$  in belite (cement A) has been investigated by inversion–recovery  $^{31}\text{P}$  MAS NMR as illustrated in Figure 3. These spectra clearly reveal that the 1.0 ppm resonance exhibits a longer spin–lattice relaxation time than the resonances constituting the broad peak in the range 10 to  $-2$  ppm. The zero-crossings for the resonances from the latter peak are slightly different and observed in the range from 0.1 to 0.2 s. A subspectrum that mainly includes a single resonance from  $^{31}\text{P}$  in belite is obtained for a recovery time of 0.2 s (cf., Figure 3). The narrow resonance from  $^{31}\text{P}$  in belite shows its zero-crossing at approximately 1.0–1.5 s, giving a subspectrum for  $^{31}\text{P}$  in alite that closely resembles the  $^{29}\text{Si}$  MAS NMR spectrum of the  $M_{\text{III}}$  form for alite.<sup>23,33</sup> Employing a deconvolution of this spectrum as the subspectrum for  $^{31}\text{P}$  in alite along with a single resonance at 1.0 ppm for  $^{31}\text{P}$  in belite allows estimation of the relative intensities for these two  $^{31}\text{P}$  species at the different recovery times by simulations of the spectra in Figure 3. This approach assumes that the individual  $^{31}\text{P}$  sites constituting the alite subspectrum exhibit the same relaxation time, which is an acceptable approximation, considering the small dispersion in zero-crossings for

these sites. The intensities from the simulations ( $M_z(t)$ ) are shown relative to the equilibrium magnetization ( $M_0$ ) by a plot of  $\ln[1 - M_z(t)/M_0]$  as a function of the recovery time ( $t$ ) in Figure 4a. The absence of a linear relationship between  $\ln[1 - M_z(t)/M_0]$  and  $t$  demonstrates that the spin–lattice relaxation is not characterized by a single-exponential relationship. Following our recent analysis of the spin–lattice relaxation for  $^{29}\text{Si}$  in alite and belite,<sup>23</sup> the  $^{31}\text{P}$  intensities are analyzed using a “stretched exponential” relationship,

$$M_z(t) = M_0[1 - (1 + \alpha) \exp(-(t/T_1')^{1/2})] \quad (1)$$

which has been derived for spin relaxation caused by paramagnetic impurities in the absence of spin diffusion.<sup>35</sup> Here,  $\alpha$  is a constant related to pulse imperfections (i.e.,  $\alpha = 1$  for an ideal  $180^\circ$  pulse) and  $T_1'$  is the time constant for the stretched exponential spin–lattice relaxation. Assuming this relationship, a satisfactory fit to the experimental  $M_z(t)$  intensities (Figure 4b) is obtained along with the  $T_1'$  spin–lattice relaxation times for  $^{31}\text{P}$  in alite and belite listed in Table 2. These data are compared with the corresponding  $^{29}\text{Si}$  spin–lattice relaxation times, determined recently for the alite and belite phases in the same cement.<sup>23</sup> For both spin nuclei it is observed that the relaxation times for the belite phase are significantly longer than those for the spins in alite. This clear resemblance in  $^{31}\text{P}$  and  $^{29}\text{Si}$  relaxation behavior strongly supports our assignment of the two types of  $^{31}\text{P}$  resonances to  $^{31}\text{P}$  incorporated in alite and belite by a substitution mechanism where  $(\text{PO}_4)^{3-}$  ions replace  $(\text{SiO}_4)^{4-}$  sites.

The simulations of the inversion–recovery  $^{31}\text{P}$  MAS NMR spectra also provide the equilibrium magnetization ( $M_0$ ) for  $^{31}\text{P}$  in alite and belite (eq 1) and thereby the molar

(34) Fyfe, C. A.; Meyer zu Altenschildesche, H.; Skibsted, J. *Inorg. Chem.* **1999**, *38*, 84–92.

(35) Tse, D.; Hartmann, S. R. *Phys. Rev. Lett.* **1968**, *21*, 511–514.

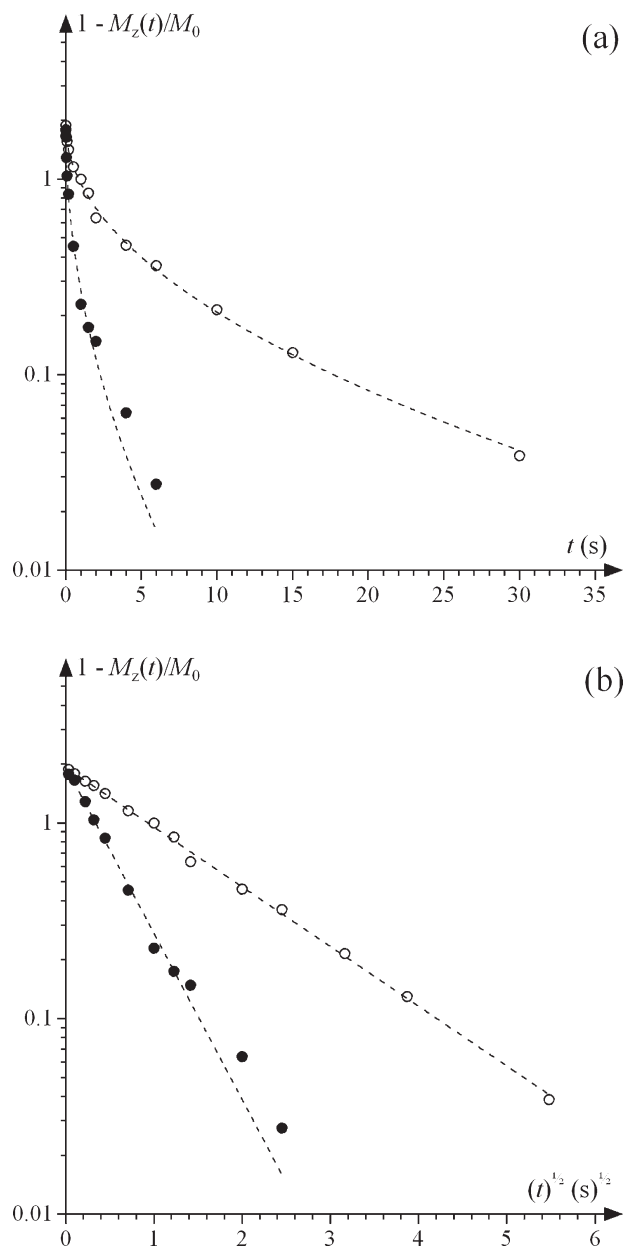


**Figure 4.** Semilog plots of  $[1 - M_z(t)/M_0]$  as a function of the recovery time  $t$  (a) and  $\sqrt{t}$  (b), which should result in linear relationships for single-exponential and stretched exponential spin–lattice relaxation processes, respectively. The graphs include data for <sup>31</sup>P in alite (filled circles) and belite (open circles) obtained from deconvolutions of the inversion–recovery <sup>31</sup>P MAS NMR spectra of cement A shown in Figure 3. The dashed curves/lines correspond to a fit of the data to a stretched exponential relationship (eq 1), resulting in the <sup>31</sup>P relaxation times in Table 2.

**Table 2.** Time Constants for the <sup>31</sup>P and <sup>29</sup>Si Spin–Lattice Relaxation ( $T_1'$ ) for Alite and Belite in Cement A from <sup>31</sup>P and <sup>29</sup>Si Inversion–Recovery MAS NMR Spectra

observed nucleus	$T_1'$ (alite) <sup>a</sup> (s)	$T_1'$ (belite) <sup>a</sup> (s)
<sup>31</sup> P	0.26	2.0
<sup>29</sup> Si <sup>b</sup>	0.24	8.2

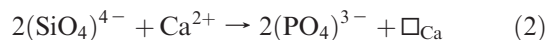
<sup>a</sup> Spin–lattice relaxation time corresponding to a stretched exponential relationship (cf., eq 1). <sup>b</sup> <sup>29</sup>Si relaxation times are from our recent study.<sup>23</sup>

ratio between <sup>31</sup>P in these two phases, i.e.,  $M_0(\text{belite})/M_0(\text{alite}) = 0.54$ . This ratio implies that the belite and

alite phases in cement A contain 0.16 and 0.29 wt % P<sub>2</sub>O<sub>5</sub>, respectively, where it is assumed that all phosphate ions (0.45 wt % P<sub>2</sub>O<sub>5</sub>) are incorporated in the silicate phases only. Combining these quantities with the bulk SiO<sub>2</sub> content (24.68 wt %) and the belite/alite intensity ratio,  $I(\text{belite})/I(\text{alite}) = 0.345$  determined from <sup>29</sup>Si NMR,<sup>23</sup> allows calculation of the degree of Si for P substitution. This results in P/Si ratios of 0.021 and 0.013 for belite and alite, respectively. These data indicate that phosphorus is preferentially incorporated in belite rather than alite with a degree of replacement corresponding to roughly 2% of the SiO<sub>4</sub> tetrahedral sites. Furthermore, these P/Si ratios are below the estimated maximum degrees of P for Si replacement in alite and belite (2.3% and 3.3%, respectively), proposed from X-ray microanalysis of laboratory-made clinkers.<sup>7</sup>

**Mechanism for Incorporation of Phosphorus in Alite and Belite.** The <sup>31</sup>P isotropic chemical shifts, the magnitudes of the <sup>31</sup>P CSAs, and the  $T_1'$  relaxation times strongly indicate that phosphorus in anhydrous Portland cements is incorporated in the alite and belite phases. A direct proof for this kind of guest-ion incorporation can potentially be achieved by the detection of the <sup>29</sup>Si resonances from alite and belite in a double-resonance <sup>31</sup>P–<sup>29</sup>Si MAS NMR experiment that utilizes the distance dependence of the <sup>31</sup>P–<sup>29</sup>Si dipolar interactions ( $\propto 1/r^3$ ) to selectively detect <sup>29</sup>Si sites in the near vicinity of the <sup>31</sup>P spins. Very recently, a similar approach has proven useful in the detection of fluoride guest ions in the alite phase of anhydrous Portland cement by <sup>29</sup>Si{<sup>19</sup>F} CP/MAS and CP-REDOR experiments.<sup>36</sup> In this work attempts have been made to characterize phosphorus in cement A by <sup>29</sup>Si{<sup>31</sup>P} CP/MAS NMR, employing a synthesized sample of Si<sub>5</sub>O(PO<sub>4</sub>)<sub>6</sub> for the setup experiments with a ramped <sup>29</sup>Si{<sup>31</sup>P} CP sequence as reported for <sup>29</sup>Si{<sup>31</sup>P} CP/MAS NMR on this model compound.<sup>37</sup> However, this experiment turned out unsuccessfully for cement A, which we ascribe to the very low concentration of (PO<sub>4</sub>)<sup>3−</sup> ions combined with the low natural abundance of <sup>29</sup>Si (4.7%) and considering the fact that only <sup>31</sup>P–<sup>29</sup>Si spin pairs with an internuclear distance less than approximately 5 Å are detected by this approach.

The observation of orthophosphate (PO<sub>4</sub>)<sup>3−</sup> units in alite and belite by replacement of (SiO<sub>4</sub>)<sup>4−</sup> tetrahedra is in agreement with the commonly suggested substitution mechanism from studies of guest ions in pure phases of alite and belite.<sup>10–14</sup> In cases where phosphorus is considered as the only element of substitution, charge balance may be achieved by creation of Ca<sup>2+</sup> ion vacancies,<sup>10,12,13</sup> i.e.,

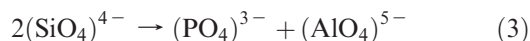


These vacancies may explain that only a small amount of phosphate can be incorporated in pure Ca<sub>3</sub>SiO<sub>5</sub>, corresponding to a maximum P/Si ratio of 0.036.<sup>9</sup> However, in commercial cements a number of other guest ions are incorporated in the calcium silicate phases, Mg, Al, Fe, S,

(36) Tran, T. T.; Herfort, D.; Jakobsen, H. J.; Skibsted, J. *J. Am. Chem. Soc.* **2009**, *131*, 14170–14171.

(37) Lejeune, C.; Coelho, C.; Bonhomme-Courty, L.; Azaïs, T.; Maquet, J.; Bonhomme, C. *Solid State Nucl. Magn. Reson.* **2005**, *27*, 242–246.

Na, K, and F being the most common elements.<sup>24</sup> This opens for coupled substitution mechanisms, where charge balance for replacement of two  $(\text{SiO}_4)^{4-}$  ions is achieved by a  $(\text{PO}_4)^{3-}$  ion and a trivalent cation. For example, it has been shown that  $\text{Al}^{3+}$  guest ions in alite and belite are present only in tetrahedral coordination,<sup>32</sup> and thus, the introduction of phosphate may promote the incorporation of aluminum in alite and belite by the substitution mechanism



The formal replacement of  $\text{Si}^{4+}$  by  $\text{P}^{5+}$  and  $\text{Al}^{3+}$  agrees well with the similarity in ionic radii for these ions, i.e., 0.40, 0.31, and 0.53 Å,<sup>38</sup> respectively. However, larger ions such as  $\text{Fe}^{3+}$  (0.79 Å) may preferentially substitute for the  $\text{Ca}^{2+}$  ions (1.14 Å), which may lead to a substitution mechanism of the type



A similar substitution mechanism was proposed in a study of the combined effect of manganese and phosphorus on the formation of monoclinic alite,<sup>10</sup> where electron paramagnetic resonance investigations revealed the presence of divalent  $\text{Mn}^{2+}$  ions in octahedral sites, suggesting a heterovalent substitution of  $(\text{SiO}_4)^{4-} + 2^{1/2}\text{Ca}^{2+}$  by  $(\text{PO}_4)^{3-} + 2\text{Mn}^{2+} + 1/2\square_{\text{Ca}}$ . It is interesting to note that the paramagnetic  $\text{Fe}^{3+}$  ions have a significant impact on the  $^{31}\text{P}$  MAS NMR spectra, as shown in Figure 2 for cements A and C. Our recent study of these cements by  $^{29}\text{Si}$  NMR revealed that alite and belite in cement C contain a higher amount of  $\text{Fe}^{3+}$  guest ions as compared to the white Portland cement (cement A).<sup>23</sup> Thus, the large number and high intensity of the spinning sidebands in Figure 2b may reflect that the  $\text{Fe}^{3+}$  ions are in the vicinity of the  $(\text{PO}_4)^{3-}$  units. This suggests that the incorporation of phosphate may potentially be charge balanced to some extent by a coupled substitution mechanism of the type given in eq 4. However, a direct pairing of the  $\text{Fe}^{3+}$  and  $(\text{PO}_4)^{3-}$  ions would most likely result in a significant loss in  $^{31}\text{P}$  NMR signal intensity as a result of the strong nuclear–electron spin dipolar interaction. A coupled substitution mechanism of the type in eq 4 may have a potential application for white Portland cement, which generally contains small amounts of  $\text{Fe}_2\text{O}_3$ , since the color of cement is strongly influenced by the amount of iron, its oxidation state, and the nature of its next-nearest neighbors.<sup>39</sup> Thus, a coupling between the  $(\text{PO}_4)^{3-}$  units and the  $\text{Fe}^{3+}$  ions may potentially shift the frequency of maximum absorption from the visible region into the UV region of the electromagnetic spectrum, as reported recently for clinkers doped with  $\text{SO}_3$ , where this shift was ascribed to the location of the  $(\text{SO}_4)^{2-}$  ions in the region of the  $\text{Fe}^{3+}$  sites.<sup>39</sup> Thereby, a controlled introduction of these guest ions in the clinkers may potentially be used to modify the color of white Portland cement.

(38) Shannon, R. D. *Acta Crystallogr.* **1976**, *A32*, 751–767.

(39) Macphee, D. E.; Duffy, J. A.; Herfort, D. *Proceedings of the 12th International Congress on Cement Chemistry*; Montreal, Canada, July 8–13, 2007, paper TH1-09.5.

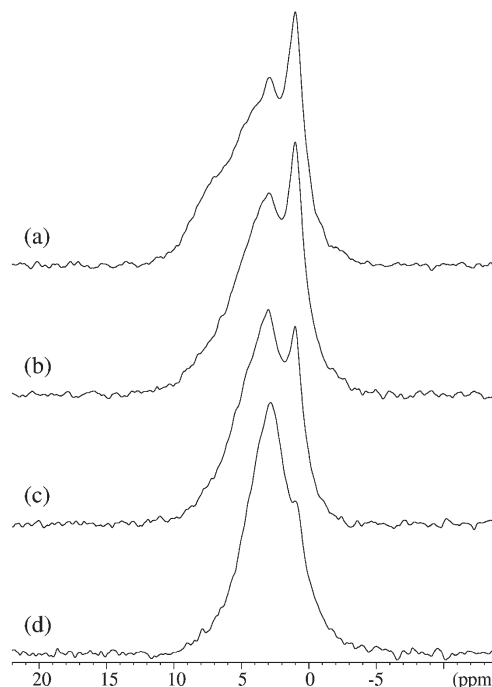


**Figure 5.**  $^{31}\text{P}$  MAS NMR spectra (9.4 T,  $\nu_{\text{R}} = 12.0$  kHz) of cement A before hydration (a) and after 1 day (b), 28 days (c), and 180 days (d) of hydration. The experiments employed a  $45^\circ$  excitation pulse, a 60 s relaxation delay, and 1000–1300 scans.

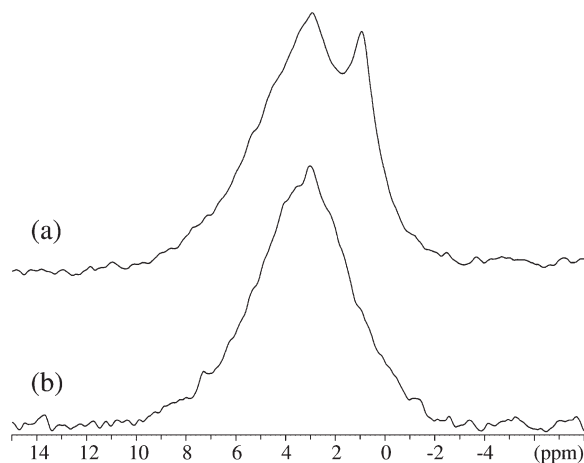


**Figure 6.** (a)  $^{31}\text{P}$  MAS and (b)  $^{31}\text{P}\{^1\text{H}\}$  CP/MAS NMR (9.4 T) of cement A after 28 days of hydration, obtained with spinning speeds of  $\nu_{\text{R}} = 12.0$  and 5.0 kHz, respectively. The spectrum in (a) is identical to the spectrum in Figure 5c. The  $^{31}\text{P}\{^1\text{H}\}$  CP/MAS NMR spectrum employed an optimum CP contact time of 1.0 ms, a 4 s repetition delay, and 16 384 scans.

**$^{31}\text{P}$  MAS and  $^{31}\text{P}\{^1\text{H}\}$  CP/MAS NMR of Hydrated Samples.** The hydration of cement A is studied by  $^{31}\text{P}$  MAS NMR (Figure 5) after 1, 28, and 180 days of hydration. At first sight, the main change in these spectra is the intensity reduction for the narrow resonance from  $(\text{PO}_4)^{3-}$  in belite after prolonged hydration. However, phosphate species with  $^1\text{H}$  in their near vicinity can be selectively detected by  $^{31}\text{P}\{^1\text{H}\}$  CP/MAS NMR, and the comparison of the  $^{31}\text{P}$  MAS and  $^{31}\text{P}\{^1\text{H}\}$  CP/MAS NMR spectra for cement A hydrated for 28 days (Figure 6) clearly reveals that the hydrous  $(\text{PO}_4)^{3-}$  species formed upon consumption of phosphorus in alite and belite have



resonances in the same spectral range as observed for  $^{31}\text{P}$  in alite. This is supported by a closer examination of the spectra in Figure 5, which shows that the high-frequency shoulder at 7 ppm (Figure 5a) has almost vanished even after 1 day of hydration, indicating the conversion of the phosphorus guest ions in alite into hydrated phosphate species. Thus, the  $^{31}\text{P}$  MAS NMR spectra indicate that the  $^{31}\text{P}$  sites in alite are partly consumed during the early hydration (Figure 5b), whereas the main reaction for phosphate in belite is observed after somewhat longer hydration times. This is fully supported by the analysis of  $^{29}\text{Si}$  MAS NMR spectra of the same hydrated cement samples, which show a degree of reaction of 39% and 85% for alite after 1 and 28 days of hydration, respectively, whereas the first clear indication of belite hydration is observed after 14 days. The degree of reaction for belite is determined to be 24% and 61% after 28 and 180 days of hydration, respectively.

The close resemblance in  $^{31}\text{P}$  chemical shift for the anhydrous and hydrated  $(\text{PO}_4)^{3-}$  species strongly suggests that the hydrated phosphate units are formed in the near vicinity of the  $\text{Ca}^{2+}$  ions and potentially also silicate sites. Moreover, the broad peak in the  $^{31}\text{P}\{^1\text{H}\}$  CP/MAS NMR spectrum (from 8 to  $-1$  ppm) shows the presence of a range of slightly different  $(\text{PO}_4)^{3-}$  environments, potentially arising from  $(\text{PO}_4)^{3-}$  ions in a disordered/amorphous phase. Thus, we assign the resonance at 3 ppm in the  $^{31}\text{P}\{^1\text{H}\}$  CP/MAS NMR spectrum to hydrated  $\text{PO}_4$  species incorporated in the disordered calcium–silicate–hydrate (C–S–H:  $(\text{CaO})_x(\text{SiO}_2)_y(\text{H}_2\text{O})_z$ ) phase, the main hydration product resulting from Portland cement hydration. The  $(\text{PO}_4)^{3-}$  ions are most likely incorporated in the C–S–H interlayers between the defect dreierketten silicate chains sandwiching a calcium–oxide layer with 7-fold coordinated  $\text{Ca}^{2+}$  ions. This assignment is based on the fact that replacement of either a chain ( $\text{Q}^2$ ) or end-group ( $\text{Q}^1$ )  $\text{SiO}_4$  tetrahedron by a  $\text{PO}_4$  unit would lead to a distinct shift of the  $^{31}\text{P}$  resonance toward lower frequency. Furthermore, this kind of  $\text{SiO}_4$  substitution would also result in a significant  $^{31}\text{P}$  chemical shift anisotropy, as generally found for pyro- and metaphosphates,<sup>16,34</sup> which is not observed in the full  $^{31}\text{P}\{^1\text{H}\}$  CP/MAS spectrum recorded with “slow-speed” spinning ( $\nu_R = 5.0$  kHz). Finally, we note that the present analysis cannot exclude that a less-ordered calcium phosphate hydrate phase, including orthophosphate units, accounts for the broadened resonance observed with a center at  $\sim 3$  ppm by  $^{31}\text{P}\{^1\text{H}\}$  CP/MAS NMR.

## Conclusions

This work has shown that  $^{31}\text{P}$  MAS NMR is a very suitable technique for studying small quantities of phosphorus in anhydrous and hydrated Portland cements, corresponding to bulk  $\text{P}_2\text{O}_5$  contents below 0.5 wt %. Two types of  $(\text{PO}_4)^{3-}$  species have been identified in the  $^{31}\text{P}$  MAS NMR spectra of the anhydrous cements. The  $^{31}\text{P}$  isotropic chemical shifts, the

magnitudes of the chemical shift anisotropies, and the  $^{31}\text{P}$  spin–lattice relaxation times determined for these sites strongly indicate that the small amount of phosphorus in anhydrous Portland cement is incorporated in the calcium silicate phases, alite and belite, by substitution of the isolated  $(\text{SiO}_4)^{4-}$  tetrahedra in these structures by  $(\text{PO}_4)^{3-}$  ions. However, a minor fraction of phosphorus may also be present in the separate phase  $\text{Ca}_3(\text{PO}_4)_2$ , as indicated by the narrow resonance at  $\delta(^{31}\text{P}) = 3.0$  ppm for two of the studied cements. The observed incorporation of  $(\text{PO}_4)^{3-}$  ions in the silicate phases is in accord with the type of substitution proposed in earlier studies of pure phases of alite and belite<sup>10–14</sup> and of laboratory clinkers.<sup>7</sup> For a white Portland cement including 0.45 wt %  $\text{P}_2\text{O}_5$ , the simulated intensities of the inversion–recovery  $^{31}\text{P}$  MAS NMR spectra combined with the calcium silicate phase analysis from  $^{29}\text{Si}$  NMR give replacements of 1.3% and 2.1% of the  $(\text{SiO}_4)^{4-}$  units by  $(\text{PO}_4)^{3-}$  ions in alite and belite, respectively, indicating a small preference for phosphorus incorporation in belite as compared to alite, even at low  $\text{P}_2\text{O}_5$  contents. A coupling between the  $^{31}\text{P}$  spins and paramagnetic centers ( $\text{Fe}^{3+}$ ) has been observed for the ordinary Portland cements, which suggests that the incorporation of  $(\text{PO}_4)^{3-}$  in alite and belite may to some extent be charge balanced by a coupled substitution mechanism where  $\text{Fe}^{3+}$  ions enter these phases by substitution for  $\text{Ca}^{2+}$  ions.

The  $^{31}\text{P}$  MAS NMR spectra of the hydrated Portland cement have revealed that the hydrated phosphate species exhibit the same chemical shifts and small chemical shift anisotropies as the  $^{31}\text{P}$  sites in alite. Thus, selective detection of these species requires the use of  $^{31}\text{P}\{^1\text{H}\}$  CP/MAS NMR. The broad resonance (from 8 to  $-1$  ppm) with maximum intensity at  $\sim 3$  ppm, observed by this experiment, is assigned to  $(\text{PO}_4)^{3-}$  ions incorporated in the interlayer region of the calcium–silicate–hydrate (C–S–H) phase, formed upon hydration of alite and belite.

The high sensitivity of  $^{31}\text{P}$  MAS NMR, combined with a range of single- and double-resonance NMR experiments, shows strong promises for the application of this approach in a range of studies focusing on phosphorus guest-ion incorporation in cement phases. Thus, this technique may be conveniently used in investigations of the applicability of alternative phosphorus-containing (bio)fuels in the production of Portland cement.

**Acknowledgment.** The use of the facilities at the Instrument Centre for Solid-State NMR Spectroscopy, Aarhus University, sponsored by the Danish Natural Science Research Council, the Danish Technical Science Research Council, Teknologistyrelsen, Carlsbergfondet, and Direktør Ib Henriksens Fond, is acknowledged. The Danish Council for Independent Research/Natural Sciences (FNU) is acknowledged for equipment grants. S.L.P. would like to thank NANOCER, a European industrial/academic partnership for fundamental research on cementitious materials, for financial support.